ISSN 0104-7760
v.26 n.1 2020

Ivanildo da Silva dos Santos[1a], Marcio Arêdes Martins[2a+], Emanuele Graciosa Pereira[2b], Angélica de Cássia Oliveira Carneiro[2c]

PHYSICAL AND THERMAL PROPERTIES OF EUCALYPTUS WOOD CHARCOAL.

SANTOS, I. S.; MARTINS, M. A.; PEREIRA, E. G.; CARNEIRO, A. C. O. Physical and thermal properties of eucalyptus wood charcoal. **CERNE**, v. 26, n. 1, p.109-117, 2020.

HIGHLIGHTS

The value of thermal conductivity obtained was 0.030 ± 0.0027 $W \cdot m^{-1} \cdot K^{-1}$.

The specific heat was 1017 ± 74 $J \cdot kg^{-1} \cdot K^{-1}$.

The apparent and bulk densities were measured as 344.6 ± 17.6 and 155.3 ± 4.1 $kg \cdot m^{-3}$, respectively.

The pressure gradient equations of Hunter, Shedd, and Hukill and Ives can model the static pressure drop across the charcoal bed.

Keywords:
Kiln
Porosity
Pressure drop
Specific heat
Thermal conductivity

ABSTRACT

The knowledge of the physical and thermal properties of eucalyptus charcoal is of fundamental importance in the design of equipment and development of cooling technologies. However, literature about physical properties for eucalyptus wood charcoal is largely unavailable, especially the thermal and aerodynamic properties, for the same material. The aim of this study was to evaluate the physical properties of eucalyptus charcoal: apparent and bulk density, pressure drop, porosity, thermal conductivity and specific heat to support the design of production and cooling systems using heat exchangers. It was found that the pressure drop could be expressed according Forchheimer's law and logarithmical empirical models, resulting in R^2 above 0.95. The apparent and bulk densities were measured as 344.6 ± 17.6 and 155.3 ± 4.1 $kg \cdot m^{-3}$, respectively, and the charcoal porosity was 54.8 ± 2%. In the investigation of flow in porous charcoal media, the pressure gradient is proportional to the increase of the superficial airflow velocity and is dependent on the charcoal bed height for low airflows and lower bed heights. However, the gradient was independent of bed height on all tests with columns larger or equal to 0.80 m. The thermal conductivity and specific heat were 0.030 ± 0.0027 $W\ m^{-1} \cdot K^{-1}$ and 1017 ± 74 $J \cdot kg^{-1} \cdot K^{-1}$, respectively.

Historic:
Received 05/12/2019
Accepted 19/02/2020

+Correspondence:
aredes@ufv.br

DOI:
10.1590/01047760202026012699

[1] Instituto Federal de Mato Grosso, Santo Antonio do Leverger, Mato Grosso, Brazil - ORCID: 0000-0002-0303-2724[a]
[2] Federal University of Viçosa, Viçosa, Minas Gerais, Brazil- ORCID: 0000-0001-5705-9431[a], 0000-0002-2642-312X[b], 0000-0003-0530-6757[c]

INTRODUCTION

The low energy potential of the Brazilian mineral coal, associated with its high import price and transport, and recent concerns over CO_2 emissions from the use of non-renewable fuels, have driven the Brazilian steel industry to use charcoal as the main bio-reducer in the production of alloys, pig iron, and steel (Pinto et al., 2018; Mousa et al., 2016). Thus, the high demand for charcoal from planted forests has driven producers to use modern techniques of production (Pereira et al., 2017; Leme et al., 2013). Among these techniques, we highlight the kilns equipped with thermometry, heat exchangers for charcoal cooling, gas burners (Cardoso et al., 2010; Carneiro et al., 2018), and wood dryers (Bustos-Vanegas et al., 2018; Rodrigues e Junior, 2019; Vilela et al., 2014; Miranda et al., 2013; Oliveira et al., 2013). Such techniques have been occurring with planning, enabling gains in charcoal productivity (Pereira et al., 2017). The artificial charcoal cooling is a promising technology in order to reduce the time of cooling in kiln systems (Oliveira et al., 2015; Bustos-Vanegas et al., 2019). Therefore, the physical properties of pressure drop, apparent and bulk densities, porosity, thermal conductivity, and specific heat of the charcoal are essential to design cooling equipment.

To determine the specific heat of granular materials, many researchers use the method of mixtures for its versatility and effectiveness (Ramaswamy et al., 2003), relating the specific heat of some agricultural products to moisture (Bitra et al., 2010; Kocabiyik et al., 2009; Aremu and Fadele, 2010) to the temperature, and to humidity and temperature (Aviara et al., 2011). There are numerous techniques for determining the thermal conductivity of materials when their measurements are based on steady state, semi-steady state, or transient conditions (Santos et al., 2010; Yyu et al., 2015). The stationary method stands out over others due to its simplicity and high degree of control for the experimental variables, generating very precise results. The disadvantage of this method refers to long observation time to reach steady state (Sadeghi, 2012), and depending on the material may change its composition like in the case of charcoal.

However, there is no recent unified information available in literature on the physical properties of charcoal produced from eucalyptus wood, constituting a scientific and technical obstacle for the design of industrial equipment used in the carbonization and post-processing of charcoal. The absence of a set of physical properties justifies the general objective of this research, which evaluated the pressure drop, apparent and bulk densities, porosity, specific heat, and thermal conductivity of charcoal. The use of transient method for determining thermal conductivity and a detailed investigation of head loss models for charcoal bed in a representative range of industrial processes are noteworthy for this study.

MATERIALS AND METHODS

Charcoal obtained from pyrolysis of eucalyptus wood (*Eucalyptus grandis)* was produced in a brick kiln (10 wood stereos capacity) with internal dimensions of 2.3 m long, 1.6 m wide, and 2.0 m tall (height) with a 0.5 m arrow at the top. The timber samples were 2.10 m long, 8 to 25 cm in diameter, and presented water content ranging from 27 to 38% d.w. (dry weight).

Carbonization conditions

In order to evaluate the physical characteristics of charcoal used in blast furnaces, the pyrolysis conditions (Table 1) were similar to those used in the kilns of the large charcoal producers (Figueiró et al., 2019).

TABLE 1 Carbonization conditions.

Parameter	Values
Wood moisture content (% d.b.)	27 - 38 %
Wood density (kg m^{-3})	490
Carbonization time (h)	70
Heating rate (oC h^{-1})	6.43
Initial temperature (oC)	150
Final temperature (oC)	450

Porosity, apparent and bulk densities of the eucalyptus charcoal

The direct method for determining the porosity of a granular mass consists of adding a fluid to the porous mass contained in a known volume container. The volume of fluid added indicates the same volume occupied by the intergranular space.

A cubic container with 60 cm edges (0.216 m^3 capacity) was used to determine the bulk density of the charcoal according to the ABNT NBR 6922 standard (1981). The mass corresponding to the total filling of the container by charcoal was measured in three replications. The bulk density was then determined using the ratio of the charcoal mass over the total volume of the container.

The apparent density was determined according to the ABNT NBR 9165 standard (1985) through fluid displacement (Equation 1). The assay was determined at 25 °C using three replicates. Where ρ_a is the apparent density ($kg \cdot m^{-3}$); m_i is the charcoal sample initial mass (kg); mf is the charcoal sample final mass (kg); ρ_w is the water density at 25 °C ($kg \cdot m^{-3}$), and V_w is the displaced volume of water (m^3).

$$\rho_a = \frac{m_i}{V_w + \frac{m_f - m_i}{\rho_w}} \quad [1]$$

The intergranular porosity (ε) of the charcoal bed is defined as the ratio of empty volume over the total volume. This property was determined indirectly from the apparent (ρ_a) and bulk density (ρ):

$$\varepsilon = 1 - \frac{\rho}{\rho_a} \quad [2]$$

Pressure drop

A volume of 0.432 m^3 charcoal with 5% water content (d.b.) with granulometry ranging from 6.35 mm to 150 mm was used for the determination of the static pressure drop. The charcoal was randomly arranged in the measuring chamber (Figure 1) to reach a height of 1.20 m. The pressure drop in the bed was measured every 0.2 m using, as reference, the static pressure in the plenum chamber for air flows of 0.15, 0.22, 0.27, 0.31, 0.34 $m^{-3} \cdot s^{-1}$ m^{-2}, which are values that match the flow rates employed for convective cooling of charcoal in the industry. Assays were performed in three replicates.

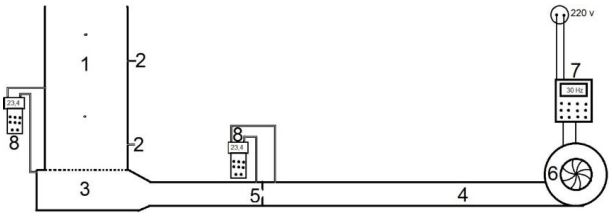

FIGURE 1 Apparatus for determining the pressure drop: (1) measuring chamber (1.20 m height and transverse area of 0.60x0.60 m2); (2) static pressure measurement points, spaced 0.20m vertically apart; (3) plenum chamber (0.3 m in height and transverse area of 0,7x0,7 m2); (4) inlet tube (3.00 m long and 0.20 m internal diameter); (5) orifice plate to measure the airflow, (6) centrifugal fan (2 hp and 1710 rpm); (7) frequency inverter (WEG CFW 10, Brazil) for airflow control; (8) micromanometer with accuracy of ± 0.1 mmca (Instrutherm, MPD- 79, Brazil).

The experimental measurements of airflow and pressure drop, expressed as a pressure gradient, were compared with the values estimated from models of Shedd (1951), Hukil and Ives (1955) and Hunter (1983), as described in Equations 3, 4 e 5, respectively. To adjust the mathematical models, non-linear regression analysis was performed, where Q" is the airflow rate ($m^3 \cdot s^{-1} \cdot m^{-2}$); a, b are constants; $\Delta p/\Delta n$ is the pressure drop per unit depth ($Pa \cdot m^{-1}$); V is the airflow rate ($m^3 \cdot s^{-1} \cdot m^{-2}$).

$$Q'' = a\left(\frac{\Delta p}{\Delta n}\right)^b \quad [3]$$

$$\frac{\Delta p}{\Delta n} = \frac{a.Q''^2}{\ln(1+bQ'')} \quad [4]$$

$$\Delta p/\Delta n = aV + bV^2 \quad [5]$$

It is important to remark that some pressure drop models consider the superficial airflow velocity (i.e., Darcy velocity or volumetric flux density), defined by the ratio between the airflow rate and the area of the cross section of the bed. However, pressure drop models like Ergun (1952) and Massarani (2002) use the intrinsic average velocity (i.e. the velocity of the interstitial flow), defined by the ratio between the superficial velocity and the porosity of the charcoal bed (ε).

Specific heat

In determining the specific heat, it was used an adiabatic calorimeter (ID 6.5 cm and 12.4 cm high). The calorimeter consists of a PVC cylinder containing, inside, a thermally insulated aluminum reservoir with polystyrene. The calorimeter was placed on a magnetic stirring plate to promote agitation of the working fluid (water). The temperature inside the calorimeter was measured by Type K thermocouples that were previously calibrated and connected to a digital thermometer (Instrutherm, TH- O96, Brazil). Charcoal samples were reduced and sieved. It was used the retained materials between ½ and ¼ mesh sieves (12.7 and 6.35 mm apertures, respectively). The use of charcoal with such particle sizes provided adequate heat exchange between the particles and water.

The heat capacity of the calorimeter (Cc) was determined by adding 100g of deionized water at 25°C to the calorimeter. Then, 100g of deionized water at 70°C was added to the calorimeter and the system was kept under agitation of 60 rpm until thermal equilibrium was reached. The heat capacity of the calorimeter was determined according to Ramaswamy et al. (2003), where C_c is the heat capacity of the calorimeter ($kJ \cdot K^{-1}$); c_w is the specific heat of water ($kJ \cdot kg^{-1} \cdot K^{-1}$); m_{hw} is the mass of hot water (kg); m_{cw} is the mass of cold water (kg); T_{eq} is the equilibrium temperature (°C); T_{cw} is the cold water temperature (°C), and T_{hw} is the hot water temperature (°C).

$$C_c = \frac{c_w\left[m_{hw}\left(T_{hw} - T_{eq}\right) - m_{cw}\left(T_{eq} - T_{cw}\right)\right]}{T_{eq} - T_{cw}} \quad [6]$$

To determine the specific heat of the charcoal, 125 g of deionized water at 25°C was added in the calorimeter. Subsequently, 25 g of charcoal at 70 °C was added to the calorimeter, and the mixture temperature was measured until thermal equilibrium was reached.

Similar to determination of the heat capacity of the calorimeter, the specific heat of the charcoal was calculated as, where c_p is the specific heat of charcoal ($J \cdot kg^{-1} \cdot K^{-1}$); m_p is the mass of charcoal (kg), and T_p is the initial temperature of charcoal (°C).

$$c_p = \frac{c_w . m_{cw}(T_{cw} - T_{eq}) + C_c(T_{cw} - T_{eq})}{m_p(T_p - T_{eq})} \quad [7]$$

Because of the natural variability of particle size charcoal, assays were performed in 10 replicates.

Thermal conductivity

Due to low mechanical strength and geometry of charcoal samples, various methodologies for determining the thermal conductivity are difficult to apply. Transient methods that consider the semi-infinite solid have been used in the experimental determination of the thermal conductivity (Kwon and Lee, 2012; Zárate et al., 2010; Mustafa et al., 2014). In the one-dimensional transient heat conduction approach, the semi-infinite solid condition (Equation 8) is valid during the initial instants of heating one side of the solid matrix. In this condition, the surface opposite to the heated surface is considered adiabatic and the temperature distribution can be written as, where erf(x) is the gauss error function; T(x,t) is the temperature at given time (°C); T_s is the surface temperature (°C); T_i is the initial point temperature (°C); φ (x,t) is the dimensionless temperature; α is the thermal diffusivity of charcoal ($m^2 \cdot s^{-1}$); and t is time (s).

$$\phi(x,t) = \frac{T(x,t) - T_s}{T_i - T_s} = erf\left(\frac{x}{2\sqrt{\alpha t}}\right) \quad [8]$$

The experiment was performed with three cylindrical samples 70 mm long and 35.5 mm in diameter. The samples were placed on a plate maintained at constant temperature (Figure 2). The cylindrical surface of the charcoal was isolated and the temperature was measured with sensors positioned 10 mm from the heated surface. The tests were performed using three heating temperatures (37.8 °C, 44.9 °C, and 48.3 °C) and three samples, totaling 9 sampling units.

To compare the means, the Tukey test was used at a 95% significance level. The mathematical model (Equation 8) was adjusted to the thermal conductivity data by means of regression analysis.

The temperature data acquisition system is composed of four T-type thermocouples, three serial data acquisition modules (LR7018, LRCOM), a converter module RS232 to RS485 to two wires (LR7520, LRCOM), and a computer. A computer program implemented on the platform C++ Builder (version 6.0) managed the

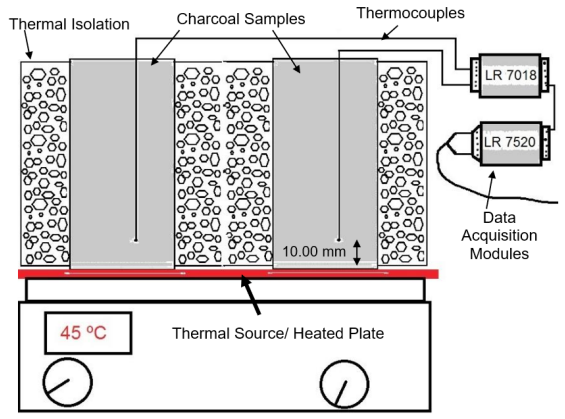

FIGURE 2 Scheme of the experimental setup with data acquisition system for determining thermal conductivity.

data acquisition system. Data received by the modules was stored on the computer in one-minute intervals.

A determining factor in transient techniques is choice of the temperature analysis interval. The data must be registered before heat flux occurs between the sample and the medium at the opposite side of the heating surface, which validates the use of the Equation 8. This time period setting was carried out following the considerations made by Santos (2002). Since the heating source has a defined thermal capacity and a contact resistance exists between the source and the sample, the initial change in temperatures with the logarithmic time scale is not linear. Therefore, this data range should not be considered in the calculation of thermal conductivity. The latter heating period should also be disregarded because linearity losses are observed for the temperature distribution in log scale, due to the heat transfer between the sample end and surroundings. This problem also mischaracterizes the semi-infinite approach (Equation 8) and therefore only the linear periods of temperature variation with time on log scale are used to determine the thermal conductivity.

RESULTS AND DISCUSSION

Porosity, pressure drop, and apparent and bulk densities

The apparent density of the charcoal was found to be 344.6 ± 17.6 kg m^{-3}. This value was lower than what was indicated by Santos et al. (2011), who found density values above 400 kg m^{-3}. However, this density parameter is strongly related to the density of the carbonized wood, which in this experiment was 490 kg m^{-3}, lower than the values reported by Santos et al. (2011) for carbonization. Pereira et al. (2016) measured

average apparent densities of 405 kg m^{-3} for the charcoal from *Eucalyptus urophylla* clones and average 361 kg m^{-3} for charcoal from *Eucalyptus camaldulensis clones*.

The bulk density of charcoal was found to be 155.3 ± 4.1 kg·m^{-3}. This value was also lower than that found by Santos et al. (2011), who measured the bulk density of charcoal for use in steelmaking to be up to 200 kg·m^{-3}.

Porosity of the charcoal calculated from the apparent and bulk densities was found to be 54.8 ± 2.7. Variations of porosity and density are acceptable since these properties depend strongly on the density of the wood used and pyrolysis operation conditions. In some porous media models (Ergun, 1952; Massarani, 2002), the intergranular porosity is used explicitly, which demonstrates the importance of its experimental determination. Lower porosity values result in greater speed for the intergranular flow and consequently larger pressure drop (Gratão et al., 2013).

In the investigation of flow in porous charcoal media, the pressure gradient is proportional to the increase of the superficial airflow velocity (Table 2) and it is a property that indicates the magnitude of the pressure drop of the fluid flow across a porous medium. The pressure gradient is dependent on the charcoal bed height for low airflows and lower bed heights. However, the gradient was independent of bed height on all tests with columns larger or equal to 0.80 m.

TABLE 2 Effect of airflow and bed height on the pressure gradient for charcoal porous medium.

Bed height (m)	Pressure gradient (Pa·m^{-1}) superficial airflow velocity ($m^3 s^{-1} m^{-2}$)				
	0.15	0.22	0.27	0.31	0.34
0.20	4.90Be	14.71Ad	26.15Ac	31.05Ab	39.22Aa
0.40	7.35ABe	19.61Ad	25.33Ac	35.96Ab	43.31Aa
0.60	9.26ABe	19.61Ad	28.33Ac	34.87Ab	43.58Aa
0.80	11.44Ae	20.02Ad	29.42Ac	38.00Ab	46.17Aa
1.00	12.09Ae	19.94Ad	29.09Ac	38.90Ab	47.72Aa
1.20	11.71Ae	21.52Ad	31.05Ac	40.04Ab	49.03Aa

Pressure gradient mean values followed by the same capital letters between rows (bedheight) and lower among columns (airflow) do not differ at 95 % probability by Tukey test.

The effect of the porous medium thickness in the pressure gradient can also be used to verify the adjustments of Shedd (1951), Hukil and Ives (1955) and Hunter (1983) models to the experimental data (Figure 3). Regardless of the model, the quality of adjustment improves with increasing height. Thus, experimental measurements using deeper charcoal beds provide better model adjustment.

From the model adjustments shown in Figure 3, the pressure gradient for the charcoal should be measured in fixed beds at heights of at least one meter. As the charcoal pieces has a high average diameter (6.07 ± 2.54) in relation to the bed height, differences in

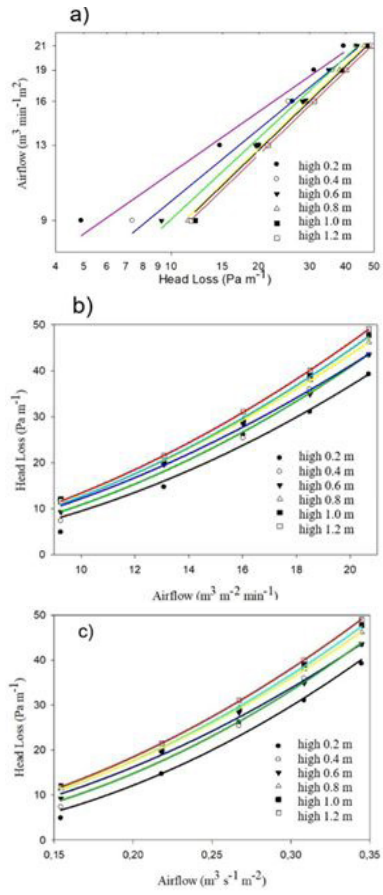

FIGURE 3 Effect of the charcoal bed height in the adjustment to the model of (a) Shedd (1951), (b) Hukill and Ives (1955), and (c) Hunter (1983) to experimental data of pressure gradient as a function of airflow speed.

tortuosity values and local porosity are more pronounced for smaller bed heights. With increasing height, these differences decrease, making the charcoal porous medium isotropic.

Considering all experimental measurements above 0.8 m, the model parameters shown in Table 3 can be estimated based on both specific and intrinsic velocity.

TABLE 3 Model adjustments for pressure gradient for charcoal porous media.

Model	Velocity	Parameter		R^2
		a	b	
Shedd (1951)	Superficial	1.861	0.561	0.997
	Interstitial	4.307	0.561	0.997
Hukil and Ives (1955)	Superficial	0.606	11.487	0.997
	Interstitial	0.182	6.273	0.997
Hunter (1983)	Superficial	21.58	343.65	0.998
	Interstitial	11.81	103.25	0.998

In cooling a bed inside a charcoal production kiln, the models written in terms of interstitial velocity are more suitable in the design of cooling systems since the interstitial velocity that percolates the charcoal particles is the limiting factor in the cooling process (Table 3). This is because the convective coefficient in the porous

medium is a function of the Reynolds number based on the diameter of the particle (Hermansson and Thunman, 2011). The models using linear and quadratic coefficients (Hunter 1983) are of direct implementation in simulation programs for computational fluid mechanics (Table 3). This attribute the term of extra stress to the fluid allowing the modeling of fluid flow in porous media.

Specific heat

The results found for the specific heat of eucalyptus charcoal ranged from 891 to 1096 $J \cdot kg^{-1} \cdot K^{-1}$, obtaining an average value 1017± 74 $J \cdot kg^{-1} \cdot K^{-1}$. The variability observed in the value of specific heat is justified by the inherent heterogeneity of charcoal samples produced in kilns. The specific heat values obtained were close to values for charcoal, as noted by Gupta et al. (2003) (768-1506 $J \cdot kg^{-1} \cdot K^{-1}$), and Eltom and Sayigh (1994) (709 $J \cdot kg^{-1} \cdot K^{-1}$).

The thermo-physical properties of charcoal can be compared to coal, an input that has a similar function to charcoal in the pig iron production chain. Wen et al. (2015) determined the thermal conductivity and specific heat capacity for bituminous coal from 25 to 300°C. The results ranged from 0.118 to 0.175 $W \cdot m^{-1} \cdot K^{-1}$ e 1025 to 2090 $J \cdot kg^{-1} \cdot K^{-1}$ for thermal conductivity and specific heat capacity, respectively.

Specific heat is the amount of heat in kilojoules required to change the temperature of 1 kg of material by 1°C. The heat released to cool the charcoal can be calculated based on the specific heat of the charcoal and the change in temperature. The dimensioning and construction of cooling systems has been taking place, taking into account basically the amount of heat that is desired to be removed from the kilns in an interval of time that justifies its implementation.

Thermal properties of woody materials are often influenced by various factors, such as the wood species, density, moisture, and fiber orientation (Larfeldt et al. 2000). The properties of wood charcoal are highly dependent on the source and the process conditions during the pyrolysis process. This fact justifies the variability in the specific heat values obtained in this research.

Thermal conductivity

Figure 4a shows that the temperature profiles are characteristic of the heating process. Initially, there is a period in which heat tends to break the contact resistance (detail, Figure 4a). Contact resistance occurs due to the contact between the thermocouple and charcoal interfaces which causes some resistance to heat transport. After this period, there is a transient period followed by a steady period with low temperature variation.

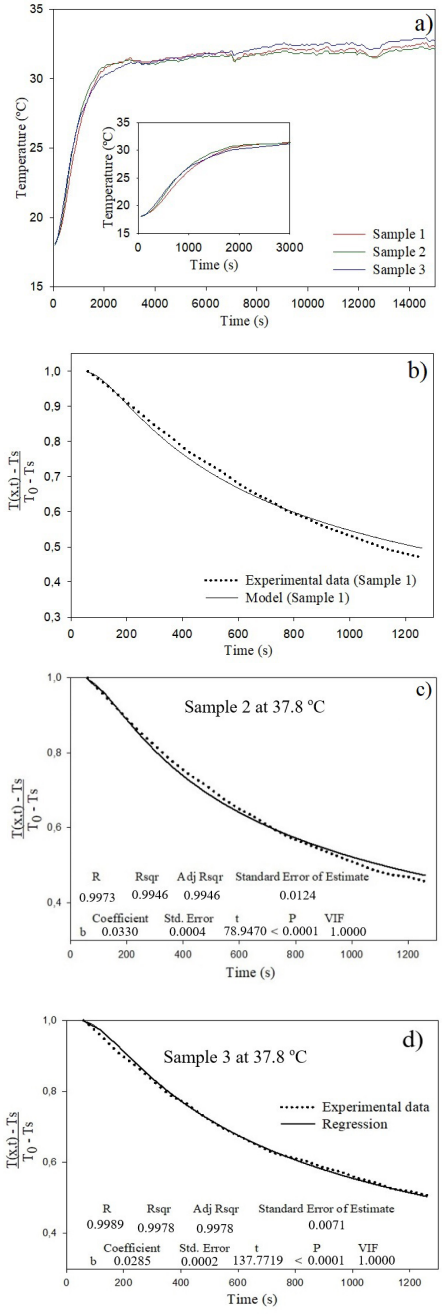

FIGURE 4 (a) Temperature distribution at 10 mm from the surface heated to 37.8°C, as a function of time, and model adjustments for samples (b) 1, (c) 2 and (d) 3.

The semi-infinite solid model (Equation 8) was fit to the experimental data for dimensionless temperature (Figure 4b to 4d) with R^2 values higher than 0.97, using the thermal diffusivity as the adjustment parameter (Table 4). Additional tests were conducted at temperatures of 44.9 and 48.3°C, performing respective adjustments to the model (Table 4).

The thermal conductivity is a characteristic parameter for measuring the ability of heat transfer.

TABLE 4 Summary of the regression analysis for the thermal conductivity (K) in the heated surface temperatures of 37.8, 44.9 and 48.3°C.

Temperature (°C)	37.8			44.9			48.3		
Sample	1	2	3	1	2	3	1	2	3
R^2	0.990	0.994	0.997	0.999	0.997	0.979	0.998	0.999	0.986
Thermal condutivity ($W \cdot m^{-1} \cdot K^{-1}$)	0.029	0.033	0.028	0.031	0.033	0.027	0.028	0.031	0.026
Standard Error	0.0005	0.0004	0.0002	0.0001	0.0003	0.0006	0.0002	0.0001	0.0005
T	59.0865	78.9470	137.7719	212.6646	121.7897	46.5795	131.5566	272.9937	54.6177
P	<0.0001	<0.0001	<0.0001	<0.0001	<0.0001	<0.0001	<0.0001	<0.0001	<0.0001
VIF	1.0000	1.0000	1.0000	1.0000	1.0000	1.0000	1.0000	1.0000	1.0000

Most lignocellulosic material has a thermal conductivity that increases with temperature; however, for surface temperatures used in this study (37.8°C, 44.9°C, and 48.3°C) this effect was not observed due to slight variation between the surface temperatures at the 5% level of significance for the F test of variance analysis (Table 5). Eltom and Sayigh (1994) found no relation between conductivity and temperature increasing in the range 30 to 90°C. Higher temperatures can be evaluated, but charcoal ignition must be considered.

TABLE 5 Thermal conductivity values charcoal for different heating temperatures.

Sample	Thermal conductivity ($W \cdot m^{-1} \cdot K^{-1}$)			
	37.8°C	44.9°C	48.3°C	Average
1	0.030±0.0005	0.031±0.0001	0.028±0.0002	0.030ab
2	0.033±0.0004	0.034±0.0003	0.032±0.0001	0.033a
3	0.029±0.0002	0.027±0.0006	0.026±0.0005	0.027b

Mean values of thermal conductivity, followed by the same letter in the column, do not differ by Tukey test at 95 % probability.

The average thermal conductivity values (Table 5), independent of temperature, showed a significant difference between the charcoal samples. This is due to the anisotropic structure of charcoal, which is characterized by internal cracks in the samples. Since the thermal conductivity variation with temperature was not significant in the tested range, the average value was 0.030 ± 0.0027 $W \cdot m^{-1} \cdot K^{-1}$, considering the average values presented in Table 4. It is noted that these results lie within the range of values published (Gupta, 2003; Eltom and Sayigh, 1994). Eltom and Sayigh (1994) found that thermal conductivity values ranged from 0.025 to 0.09 $W \cdot m^{-1} \cdot K^{-1}$ in a temperature range from 30 to 90°C for charcoal. Gupta et al. (2003) obtained values of 0.0946 $W \cdot m^{-1} \cdot K^{-1}$ at a temperature of 35°C for charcoal particles from low density wood. It is noteworthy that the above authors did not describe what kind of wood was used for carbonization tests.

Thermal conductivity of materials is a function of the solid fraction composition and its microstructure (Vivaldini et al., 2014). The structure of charcoal is partly the result of the wood structure and partly of the structural changes during pyrolysis, which in turn depends on main parameters of the carbonization, such as temperature, heating rate, carbonization time and pressure. It is therefore difficult to predict the structural changes during pyrolysis, and the pore size distribution is likely to vary between samples. This leads to unavoidable uncertainties in modelling of the effective thermal conductivity and, as a consequence, difficulties in determining the thermal conductivity and specific heat (Larfeldt et al., 2000).

The heat transfer properties of charcoal (thermal conductivity and specific heat) are important for modelling of the pyrolysis of wood and the process of charcoal cooling, investigating the kinetics of the self-heating phenomena due to charcoal oxidation (Bustos-Vanegas et al., 2019); and understanding heat transfer and its inertia in the structural components of the kiln (Bustos-Vanegas et al., 2018).

In this context, advanced computer modeling and simulation techniques can assist in the development of new methodology for cooling of charcoal, system performance evaluation, determination of the viability of its commercial application and process optimization.

CONCLUDING REMARKS

The models of Hunter, Shedd, and Hukill and Ives can also be used for modelling the dependency of the static pressure drop with the airflow velocity across the charcoal bed, and they are valid for beds deeper than 0.8 m.

The apparent and bulk densities are in the required range for steelmaking using; The porosity and specific surface area for the charcoal showed good characteristics and little variation.

The calorimeter mixing method can be used to measure the specific heat of the eucalyptus wood charcoal since the variations between the samples were small. The semi-infinite solid approach can be used for charcoal thermal conductivity determination, since good agreement to experimental data were verified. The importance of evaluating the time interval is also highlighted, in which the model is also valid. The joint determination of pressure gradient model, apparent and bulk densities, porosity and surface area, specific heat, and thermal conductivity for the same batch of charcoal allows the studies of fluid flow, heat and mass transfer

in porous media for many industrial applications such as cooling, carbonization, power and heat generation.

REFERENCES

AREMU, A. K.; FADELE, O. K. Moisture Dependent Thermal Properties of Doum Palm Fruit (Hyphaene Thebaica). **Journal of Emerging Trends in Engineering and Applied Sciences**, v. 1, n. 2, p. 199 – 204, 2010.

ASSOCIAÇÃO BRASILEIRA DE NORMAS TÉCNICAS - ABNT. **NBR 9165:** Carvão vegetal: Determinação da densidade relativa aparente, relativa verdadeira e porosidade - Método de ensaio. Rio de Janeiro, 1985.

ASSOCIAÇÃO BRASILEIRA DE NORMAS TÉCNICAS - **ABNT. NBR 6922:** Carvão vegetal: determinação da massa específica (densidade a granel). Rio de Janeiro, 1981. 2 p.

AVIARA, N. A.; EHIABHI, S. E.; AJIBOLA, O. O.; ONI, S. A.; POWER, P. P.; ABBAS, T.; ONUH, O. A. Effects of moisture content and temperature on the specific heat of soya bean, Moringa oleifera seed and Mucuna flagellipes nut. **International Journal of Agricultural and Biological Engineering**, v. 4, n. 1, p. 87-92, 2011.

BITRA, V. S. P.; BANU, S.; RAMKRISHNA, P.; NARENDER, G.; WOMAC, A. R. Moisture dependent thermal properties of peanut pods, kernels, and shells. **Biosystems Engineering**, v. 106, p. 503-512, 2010.

BUSTOS-VANEGAS, J. D.; MARTINS, M. A.; CARNEIRO, A. C. O.; FREITAS, A. G.; BARBOSA, R. C. Thermal inertia effects of the structural elements in heat losses during the charcoal production in brick kilns. **Fuel**, v. 226, p. 508-515, 2018.

BUSTOS-VANEGAS, J. D.; MARTINS, M. A.; FREITAS, A. G.; MELLMANN, J. Experimental characterization of self-heating behavior of charcoal from eucalyptus wood. **Fuel,** v. 15, p. 412-418, 2019.

CARDOSO, M. T. et al. Construção de um sistema de queima de gases da carbonização para redução da emissão de poluentes. **Cerne**, v. 16, p. 115-124, 2010.

CARNEIRO, A. DE C. O. et al. Monitoring of transportation network of carbonization gases in cogeneration projects. **Revista Arvore**, v. 42, 2018.

ELTOM, O. M. M.; SAYIGH, A. A. M. A simple method to enhance thermal conductivity of charcoal using some additives. **Renewable Energy**, v. 4, p. 113-118, 1994.

ERGUN, S. Fluid flow through packed columns. **Chemical Engineering Progress**, v. 48, p. 89-94, 1952.

FIGUEIRÓ, C. G.; CARNEIRO, A. C. O.; SANTOS, G. R. et al. Caracterização do carvão vegetal produzido em fornos retangulares industriais. **Revista Brasileira de Ciências Agrárias - Brazilian Journal of Agricultural Sciences**, v.14, n.3, p. 56-59, 2019.

GRATÃO, P. T. DA S. et al. Perda de pressão estática em uma coluna de grãos de quinoa. **Revista Brasileira de Engenharia Agrícola e Ambiental**, v. 17, 2013.

GUPTA, M.; YANG, J.; ROY, C. Specific heat and thermal conductivity of softwood bark and softwood char particles. **Fuel**, v. 82, p. 919-927, 2003.

HERMANSSON, S.; THUNMAN, H. CFD modelling of bed shrinkage and channelling in fixed-bed combustion. **Combustion and Flame**, v. 158, p. 988-999, 2011.

HUKILL, W. V.; IVES, N. C. Radial air flow resistance of grain. **Agricultural Engineering**, v. 36, p. 332-5, 1955.

HUNTER, A. J. Pressure difference across an aerated seed bulk for some common duct and store cross sections. **Journal of Agricultural Engineering Research**, v. 28, p. 437-50, 1983.

KOCABIYIK, H.; KAYISOGLU, B.; TEZER, D. Effect of moisture content on thermal properties of pumpkin seed. **International Journal of Food Properties**, v. 12, n. 2, p. 277-285, 2009.

KWON, S. Y.; LEE, S. Precise measurement of thermal conductivity of liquid over a wide temperature range using a transient hot-wire technique by uncertainty analysis. **Thermochimica Acta**, v. 542, p. 18– 23, 2012.

LARFELDT, J.; LECKNER, B.; MELAAEN, M. C. Modelling and measurements of heat transfer in charcoal from pyrolysis of large wood particles. **Biomass and Bioenergy**, v. 79, p. 1637-1643, 2000.

LEME, M. M. V.; VENTURINI, O. J.; LORA, E. E. S, et al. Electricity generation from pyrolysis gas produced in charcoal manufacture: Technical and economic analysis. **Journal of Cleaner Production**, v. 194, p. 219-242, 2018.

MASSARANI, G. **Fluidodinâmica em Sistemas Particulados**. E- Papers, 2002. 152p.

MIRANDA, R. C.; BAILIS, R.; VILELA, A. O. Cogenerating electricity from charcoaling: A promising new advanced technology. **Energy for Sustainable Development**, v. 17, p.171-176, 2013.

MOUSA E, WANG C, RIESBECK J, LARSSON M. Biomass applications in iron and steel industry: An overview of challenges and opportunities. **Renew Sustainable Energy Reviews**, v. 65, p. 1247-1266, 2016.

MUSTAFA, M. T.; ARIF, A. F. M.; MASOOD, K. Approximate analytic solutions of transient nonlinear heat conduction with temperature-dependent thermal diffusivity. **Abstr Appl Anal**., 2014.

OLIVEIRA, A. C.; CARNEIRO, A. C. O.; BARCELLOS, D. C.; RODRIGUEZ, A. V.; AMARAL, B. M. N.; PEREIRA, B. L. C. Resfriamento artificial em fornos retangulares para a produção de carvão vegetal. **Revista Árvore**, v. 39, n. 4, p. 769-778, 2015.

OLIVEIRA AC, CARNEIRO A DE CO, PEREIRA BLC, et al. Otimização da produção do carvão vegetal por meio do controle de temperaturas de carbonização. **Revista Árvore**, v. 37, n. 3, p. 557-566, 2013.

RAMASWAMY, H.; RAGHAVAN, V.; CHAKRAVERTY, A.; MUJUMDAR, A. **Handbook of Postharvest Technology**. CRC Press, 2003. 912p.

PEREIRA, E. G.; MARTINS, M. A.; PECENKA, R.; CARNEIRO, A. D. C. O. Pyrolysis gases burners: Sustainability for integrated production of charcoal, heat and electricity. **Renewable and Sustainable Energy Reviews**, v. 75, p. 592-600, 2017.

PEREIRA, B. L. C.; CARVALHO, A. M. M. L.; OLIVEIRA, A. C.; SANTOS, L. C.; CARNEIRO, A. C. O.; MAGALHÃES, M. A. Efeito da carbonização da madeira na estrutura anatômica e densidade do carvão vegetal de eucalyptus. **Ciência Florestal**, v. 26, n. 2, p. 545-557, 2016.

PINTO, R. G. D.; SZKLO, A. S.; RATHMANN, R. CO_2 emissions mitigation strategy in the Brazilian iron and steel sector–From structural to intensity effects. **Energy Policy**, v. 114, p. 380-393, 2018.

RODRIGUES, T.; BRAGHINI, JUNIOR, A. Charcoal: A discussion on carbonization kilns. **Journal of analytical and applied pyrolysis** , v. 143, p. 104670, 2019.

SADEGHI, A. Thermal conductivity of feed pellets. **Journal of Agricultural Science and Technology**, v. 14, p. 975–984, 2012.

SANTOS, R. C.; CARNEIRO, A. C. O.; CASTRO, A. F. M. CASTRO; R. V. O.; BIANCHE, J. J.; SOUZA, M. M. S.; CARDOSO, M. T. Correlações entre os parâmetros de qualidade da madeira e do carvão vegetal de clones de eucalipto. **Scientia Forestalis**. v. 39, n. 90, p. 221-230, 2011.

SANTOS, W. N. O método de fio quente: técnica em paralelo e técnica de superfície. Cerâmica, v. 48, n. 306, p. 86-91, 2002.

SANTOS W. N.; SANTOS J. N.; MUMMERY, P.; WALLWORK, A. Thermal diffusivity of polymers by modified angström method. **Polymer Testing**, v. 29, p. 107-112, 2010.

SHEDD, C. K. Some new data on resistance of grains to air flow. **Agricultural Engineering**, v. 32, p. 493-5, 1951.

VILELA, A. O.; LORA, E.S.; QUINTERO, Q. R.; VICINTIN, R. A.; SOUZA, T.P.S. A new technology for the combined production of charcoal and electricity through cogeneration. **Biomass Bioenergy**, v.69, pp. 222-240, 2014.

VIVALDINI, D. O. et al. Revisão: Fundamentos e materiais para o projeto da microestrutura de isolantes térmicos refratários de alto desempenho. **Ceramica**, v. 60, n. 354, p. 297–309, 2014.

WEN, H. et al. Temperature dependence of thermal conductivity, diffusion and specific heat capacity for coal and rocks from coalfield. **Thermochimica Acta**, v. 619, p. 41–47, 2015.

YU, D. U.; SHRESTHA, B. L.; BAIK, O. D. Thermal conductivity, specific heat, thermal diffusivity, and emissivity of stored canola seeds with their temperature and moisture content. **Journal of Food Engineering**, v. 165, p. 156–165, 2015.

ZÁRATE, J. M. O.; HITA, J. L.; KHAYET, M.; LEGIDO, J. L. Measurement of the thermal conductivity of clays used in pelotherapy by the multi-current hot-wire technique. **Applied Clay Science**, v. 50, p. 423–426, 2010.